5-2017

Improving Water Barrier Properties of Epoxy Coatings with Addition of Graphene Oxide

Sang H. Kim
College of William and Mary

Improving Water Barrier Properties of Epoxy Coatings with Addition of Graphene Oxide

Sang Hoon Kim

Bachelor of Science, the College of William and Mary 2017

A thesis submitted in partial fulfillment of the requirement
for the degree of Bachelor of Science in Chemistry from
The College of William and Mary

Department of Chemistry

The College of William and Mary

2017

Approval Page

This thesis is submitted in fulfillment of the requirements for Honors in Chemistry;

Bachelor of Science Degree

Sang Hoon Kim

Approved by the Committee, May, 2017

Committee Chair
David Kranbuehl, Chemistry
The College of William and Mary

Christopher Abelt, Chemistry

Dana Lashley, Chemistry

Hannes Schniepp, Applied Science

Williamsburg, VA

Abstract

Epoxy coating paint is commonly used in metal coatings in aircraft and marine constructions due to its excellent mechanical properties and chemical resistance. However, being in a harsh environment, they are susceptible to degradation by water which significantly reduces the lifetime of the coatings. To better protect the material from corrosion, stress, degradation and absorption of water, nanofillers can be incorporated to improve the barrier properties. This paper explores the effect of incorporating graphene oxide (GO) as a nanofiller and the effect of different functionalization and surface modification of graphene oxide on reducing the water vapor permeability and water absorption of the epoxy film. There seemed to be no detectable effect of different weight loadings of the GO. A better dispersion by sonication method seemed to have greater effect than having the bigger aspect ratio of the nanoparticles. The effect of functionalization of GO with diethylene-triamine and butyl-amine showed the greatest effect on reducing the water vapor transmission compared to the reduced GO.

Acknowledgements

Professor David Kranbuehl

John-Andrew Samuel Hocker

Mahmoud Amin

Professor Christopher Abelt

Professor Dana Lashley

Professor Hannes Schniepp

Chemistry Department at the College of William and Mary

Roy Charles Center

Friends, Family, and Colleagues in the Lab.

Table of Contents

Chapter Page Number

1. Introduction

Epoxy resins are a class of reactive polymers that have excellent mechanical strength, thermal and chemical resistance. Epoxy has a wide range of applications due to their strong adhesive properties, ease of processing, and water resistance. These include metal coatings in aircrafts and ships, marine construction, use in electronics, high tension electrical insulators, and other paint manufacturing. Due to its versatile nature, epoxy is replacing many other conventional materials used in boats and various underwater applications.

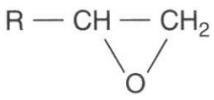

Figure 1. Molecular structure of epoxide group.

Epoxy resins are thermosetting polymers and defined as a molecule containing more than one epoxide groups, as shown in Fig.1, epoxies generally react or cross-link either with themselves through catalytic polymerization or with a wide range of co-reactants including amines, acids, phenols, alcohols etc. These co-reactants are often referred to as hardeners or curatives and the cross-linking reaction is commonly referred to as curing.

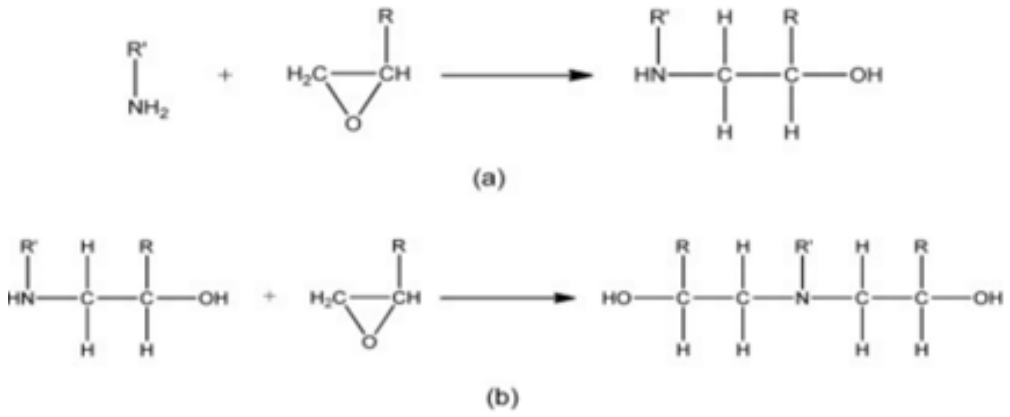

Fig. 2 General reaction of two-part Epoxy paint

Primary amines undergo an addition reaction and ring opening reaction with the epoxide group to form a hydroxyl group and a secondary amine.[27]

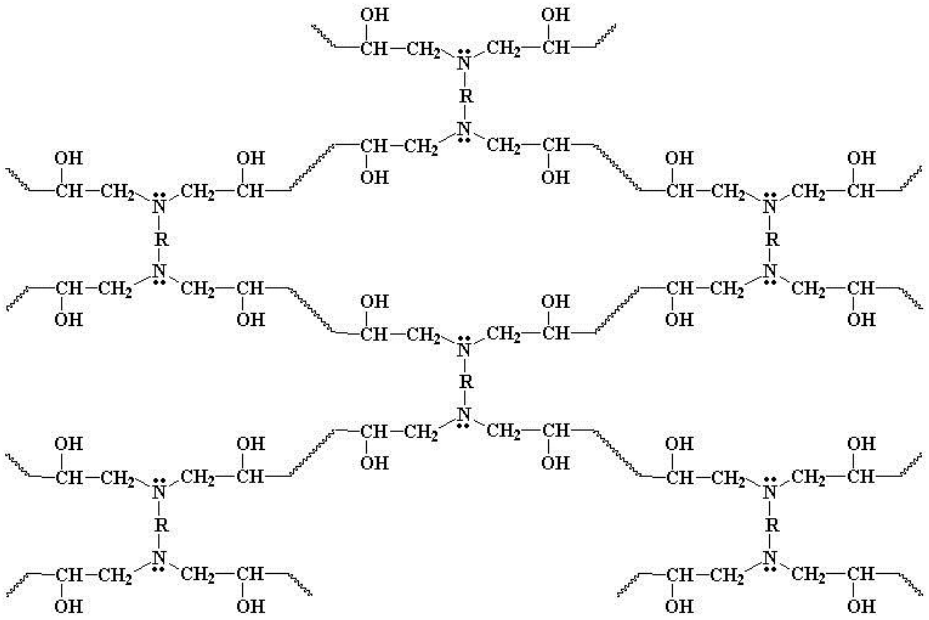

Fig. 3 Structure of cross-linked epoxy coating

The secondary amine can further react with an epoxide to form a tertiary amine and form a highly cross-linked, three-dimensional network as shown in Fig.3

Despite its exceptional properties, the harsh environment that paint is under, makes the epoxy paint still suffer from degradation and water absorption causing the paint to swell and come off the material. Moreover, they are susceptible to mechanical and thermal stress, which can deform the surface and break the epoxy coating. To better protect the material from corrosion, stress, degradation and absorption of water, nanofillers can be incorporated to improve the barrier properties.

When successful, ship building companies and navy can use fewer coatings, add less weight to the ship, save costs, and increase efficiency and lifetime, as they require tons of paint to repaint its ship from a 5 to 10 year interval.

Barrier performance has become important for many industries ranging from food packaging, medical to electronic industries.[17-21] Materials that are vulnerable or sensitive to moisture or certain gases certainly demand enhanced barrier performance from the material. Polymers are often used in these industries due to their high protection performance, functionality, lightweight, ease of processing and low cost. Moreover, they provide high mechanical strength, thermal and chemical stability that are desired for many applications.

Despite the polymer's versatility, they are still few drawbacks such as their inherent permeability and degradation. There are numerous methods for improving barrier properties in polymers that were developed in the last decades. To enhance the barrier properties of polymers, the inclusion of impermeable fillers can significantly

enhance the barrier properties of the polymers. To improve the barrier properties of polymers, generally nonporous nanomaterials have been added to the polymer matrix as a filler to block gas, vapor or water diffusion. Without the incorporation of some kind of the nanofillers, molecules will permeate through the polymer in a shortest pathway that is perpendicular to the polymer film orientation. But these nanofillers can increase the tortuosity, which ultimately results in an extended travelling pathway of the diffusing molecules through the polymer nanocomposites.[1] Nanomaterials were used as a filler improve the properties of the barrier because the nanomaterials have exceptionally high surface area-to-volume ratio which gives rise to exceptional properties in the new products. Thus, with the aspect ratio being high, the addition of a small weight percentage of nanomaterials can have large effect on properties with negligible increase in weight.[2] Traditionally clay was widely used for barrier applications for their high aspect ratio and their compatibility with various polymers. [15,16] However, despite their attempts of improving the performance, clay based polymer nanocomposites showed a limitation due to their tendency to aggregate easily resulting in decreased barrier properties.[2] While searching for better material, graphene recently has gained the attention due to its exceptional properties.

Interest in the incorporation of single-layer graphene or functionalized graphene into polymers has become increasingly widespread due to its unique properties. Graphene is a single-layer honeycomb lattice of carbon atoms in a sp^2 hexagonal bonding configuration. Compared with other nanomaterials, graphene is structurally unique, whereas the lateral dimensions of graphene are up to tens of micrometers or larger, and the thickness is at the atomic scale.[3] Although it is only one atom thick,

graphene's pi-orbitals forms a dense delocalized cloud that blocks the gap within its aromatic rings that will aid in barrier properties.[2] Graphene is known one of the strongest material ever measured, with a Young's modulus of 1 TPa.[3] Ideally, defect free single crystalline monolayer not only has good mechanical properties, electrical conductivity, high surface area, low cost, but also has impermeability to gases. Nanocomposites based on these materials feature significant property improvements even when less than 1% of nanoparticles based on single-layer graphene are added. Moreover, many studies show that even as low as 1% loading of GO, the properties were enhanced by many fold. [10]

Filler that has good compatibility with polymer matrix usually reduces the permeability, mainly because of the reduction of the transport cross section and the increase in the tortuous paths for gas molecules.

Although graphene has some exceptional properties, it has some few setbacks. Graphene sheets with a high specific surface area tend to form irreversible agglomerates or even restack to form graphite through pi-pi stacking and van der Waals interactions if the sheets are not well separated from each other.[2] This also affects its compatibility of the graphene and the polymer matrix. The permeating molecules then can travel through the narrow gap of the relatively permeable polymer matrix rather than being impermeable with graphene. The graphene also suffers from the fact that polymer and graphene have poor interactions;[3] the polymer chains do not tightly bind with the graphene nanosheets and therefore forms a narrow gap surrounding the graphene nanosheets leaving breach pathways for molecules to travel through. Thus, it would be

ideal to form a defect free graphene that would form no holes that is well-compatible with the polymer.

Ideally, defect-free, single-crystalline, monolayer graphene has not only excellent mechanical properties and but has impermeability even to some gases. However, the synthesis of large-area, defect-free, single-crystalline, monolayer graphene is still extremely challenging.

One strategy is to use graphene oxide, GO, and its reduced form. GO consists of oxygen-containing functional groups and it can be well-dispersed in aqueous polar solvents such as water; this can lead to easier production. [3] Unfortunately, GO is significantly affected by relative humidity because of its hydrophilic nature and is also affected by thermal shock, even at low temperatures, because of its structural metastability.[2] So thin-film GO layers should be chemically or thermally reduced to prevent or minimize water vapor transmission or water absorption on the surface.

The properties of polymer nanocomposites depend strongly on how well the fillers are dispersed. The influence of graphene and its derivatives on the barrier properties of polymer nanocomposites differs by different processing methods.[2] But ultimately, homogenous dispersion of the fillers will be important for enhancing barrier properties. It is also important to note that barrier properties of graphene/polymer composites are also affected strongly by the aspect ratio and orientation of the graphene nanosheets as well as the graphene nanosheets/polymer interface and the crystallinity of the polymer matrix. Homogeneous dispersion in the polymer matrix can be achieved due to the increased interfacial adhesion between GO nanosheet and polar polymer matrix.[7] This can be accomplished by control of chemical functionalization on

the GO plane which is essential to obtain a more compatible and enhanced nanocomposite system.[6] The functionalization of the surface of the nanoparticles would increase the intermolecular forces between the polymer and the nanoparticles. The resulting effect of this better interaction would restrict the mobility of the polymer chain itself which can further inhibit the rate of diffusion of small molecules.

Regarding the effects of the functionalization of the graphene, one study found that highly functionalized GO achieved better enhancement than a low functionalized GO.[8] Greater number of oxygen-containing functional groups formed on the graphene surface were found to result in a more homogeneous dispersion of completely exfoliated graphene nanosheets by preferentially forming a strong interaction with ethylene vinyl alcohol copolymer matrix.[10] They even showed that despite the higher number of defects on graphene caused by highly functionalized groups, as well as lower aspect ratio induced by severe oxidation and sonication treatment, the highly functionalized GO gave rise to higher level of barrier performance.[7] They concluded that based on their result, the morphological structure of exfoliation and dispersion state for the graphene nanosheet in the polymer matrix is a more significant factor for producing high-performance nanocomposite than the structure of the graphene itself such as particle sizes or forming a defect-less graphene.[10]

Regarding gas barrier properties of GO loaded polymers: Nishino, M [11] determined that incorporation of GO into polymethyl methacrylate (PMMA) at a loading of 1 weight % reduced the oxygen gas transmission through the PMMA film by 50 %. Zhu, Lim [12] incorporated reduced GO from loadings ranging from 1 to 30 weight % and reduced the oxygen transmission rate as high as 93 %. Jin, J [13] incorporated

functionalized GO into Nylon (polyamide 11 & 12) at 0.3 weight % loading and Shim, S [137] incorporated functionalized GO into PET (polyethylene terephthalate) at 3 weight % loading and have achieved 47% and 97% reduction in oxygen transmission rate respectively. Kim, H [14] used reduced GO mixed with PVA (polyvinyl alcohol) composites at low weight % loading ranging from 0.07 to 0.3 and recued the oxygen gas transmission rate up to 99%. From this review, it is clear that gas permeability are improved but the properties vary according to the types of polymer used, different surface chemistry of the graphene oxide, and different weight loadings of the GO.

The barrier properties of graphene have been of widely studied and is of great interest for many potential applications. Also, techniques to improve graphene's degree of exfoliation, dispersion, and orientation in a polymer matrix while also maintaining the other advantages of both graphene and the polymer for graphene/polymer nanocomposites are still being studied. Thus it is important to have good understanding of these graphene based nanocomposite and to manipulate these exceptional properties and utilize these inexpensive carbon materials to solve the challenges faced today.

In order to understand the molecular interaction between the GO and the polymer, different types of GO-epoxy coating films were synthesized at a very low weight percent GO loadings: 0.01, 0.05, 0.10 % weight. In this research we hope to find differing effect on performance properties of different types of functionalization of GO surface.

2. Materials and Experimental Methods

2.1. GO synthesis and dispersion

GO was obtained by the synthesis procedure of Hummers.[22] Dry GO flakes were massed and were put into different solvents to see how well it disperses. First, we put the massed GO into deionized water (dI water) and into butanol. It was bath sonicated in water using a Fischer Scientific FS110D sonicator for 30 minutes to obtain a homogeneous GO-dI water and GO-butanol dispersions. Different methods of dispersion were adopted hoping to retain bigger sizes of GO and compare between the two methods of mixing and see if the GO particle size had an effect on the water vapor transmission. This second method of mixing was done by stirring the mixture over the stir plate for overnight. It resulted in similar dispersion but with a bigger particle sizes.

2.2. GO-Butyl-amine-Functionalization / GO-DETA Functionalization

Butyl-amine solution was added to a GO-butanol dispersion at a ratio of 1:1 of GO by weight at a room temperature. The butyl-amine reacted with the GO which resulted in darkening of the solution and the solution mixed over a stir plate to retain an even dispersion, designated fGO.

For Diethylene-Triamine (DETA) functionalization, a GO-butanol dispersion was kept stirring and DETA solution was mixed with 1:1 weight ratio of DETA to GO under 60^{o} C water bath. The solution turned to black and seemed to be reduced. The solution was designated as DETA-fGO.

2.3 GO-Reduction

For GO reduction, the following method was used: 100 microliters of Hydrazine hydrate was added to a 20 mL of GO-dI water mixture in pressure vial. The vial was microwaved with CEM Discovery 908005 Microwave with power of 300 Watts at 150 psi, with a max temperature limit at 180 C^o. Two different times were used: 200 seconds (half reduced, designated HrGO) and 400 seconds (fully reduced, designated FrGO). Note that the term half reduced and full reduced only refers to the relative time spent in microwave. Microwaving the mixture with hydrazine hydrate added resulted in GO particles precipitating to the bottom and becoming hydrophobic. The now reduced GO were dried in the oven, and were tested for TGA analysis to confirm less percent weight loss compared to GO. It was then re-dispersed in butanol to be put into the epoxy system.

As it was inconvenient to work with small amounts of GO while using the CEM discovery microwave, we moved on to a simpler method that allowed us to work with larger batch. A commercial microwave was used at operation power setting of 1000 W. The GO-dI water mixture was mixed with hydrazine hydrate, and were microwaved in 3 cycles for HrGO (1 cycle being 10 seconds of high microwave power and 20 seconds of stirring), and 6 cycles of the same procedure for FrGO. The now reduced GO samples were dried in a vacuum oven and were re-dispersed in butanol.

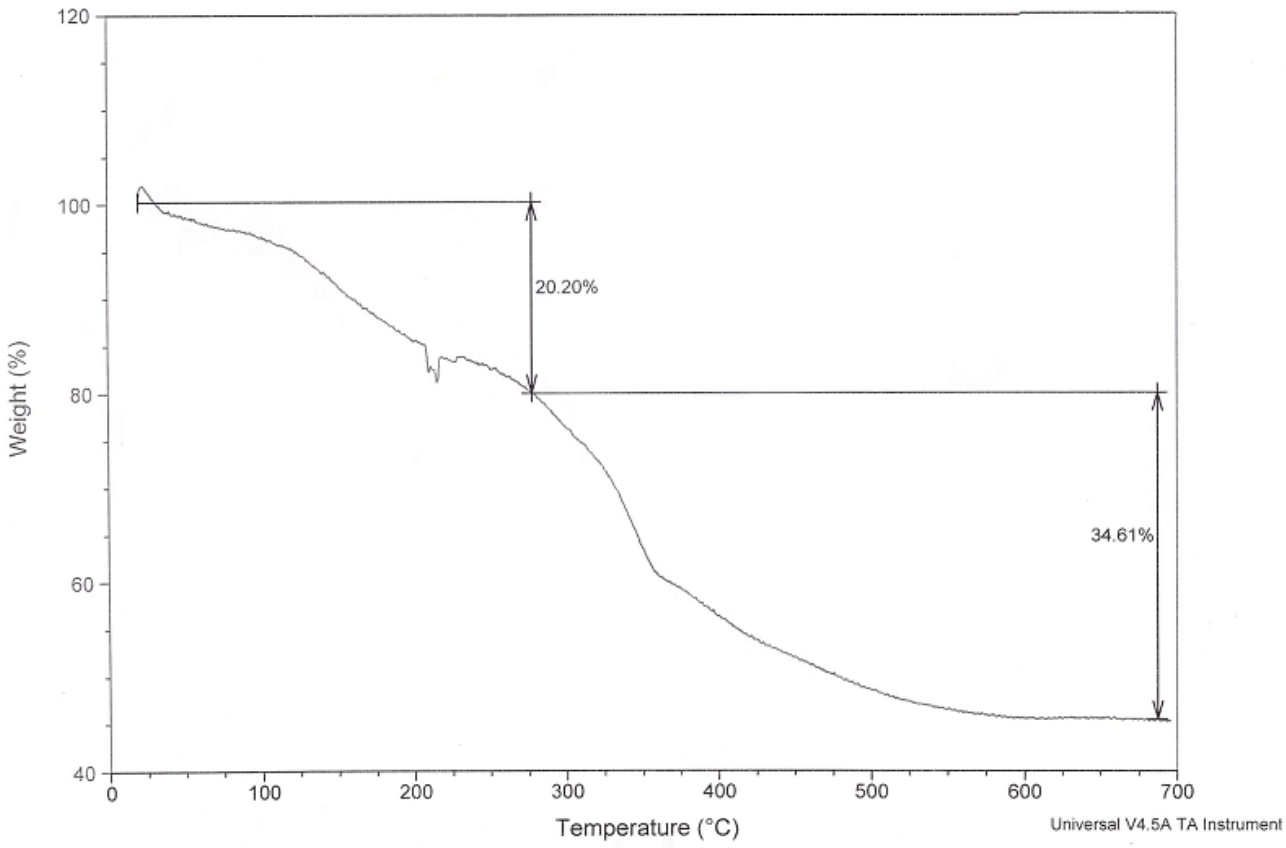

Figure 4. TGA analysis of graphene oxide (GO) flakes (~55% weight loss)

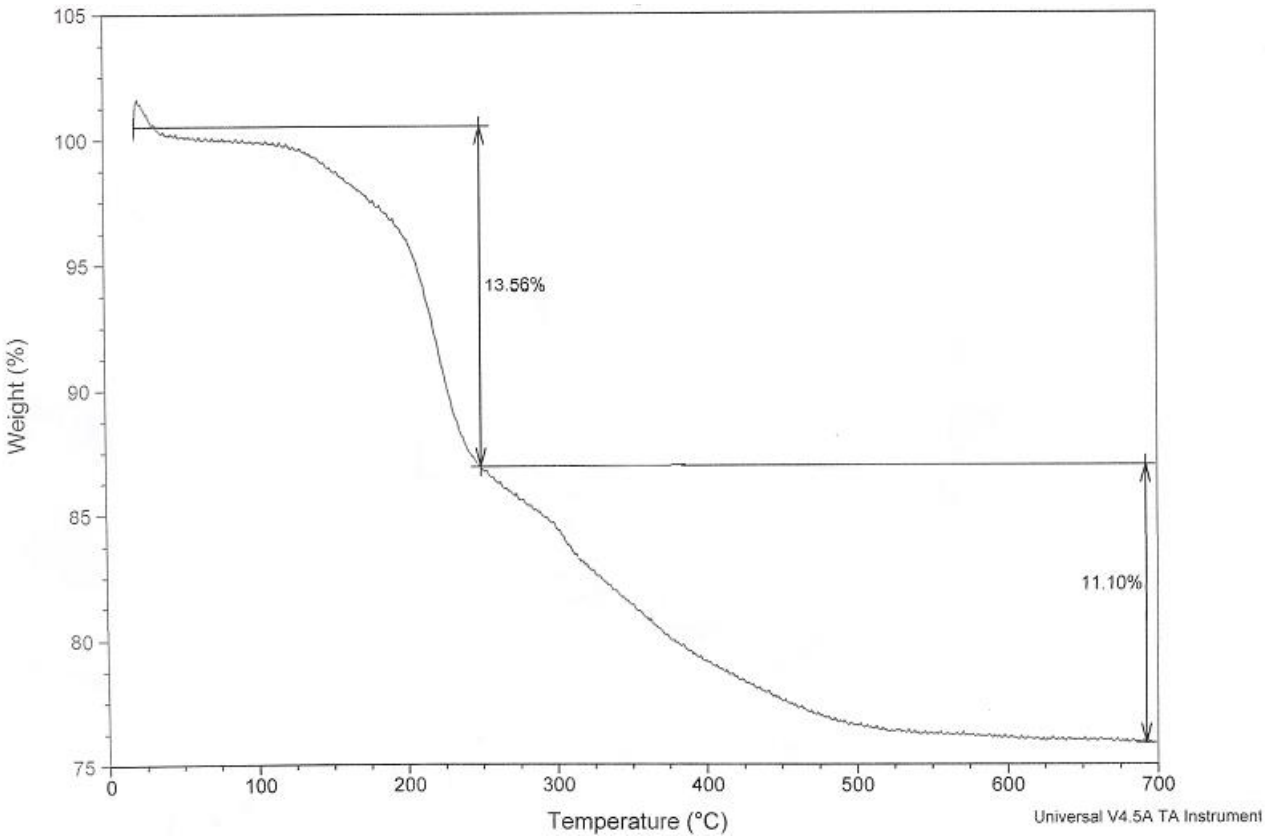

Figure 5. TGA analysis of half reduced GO (~ 25% weight loss)

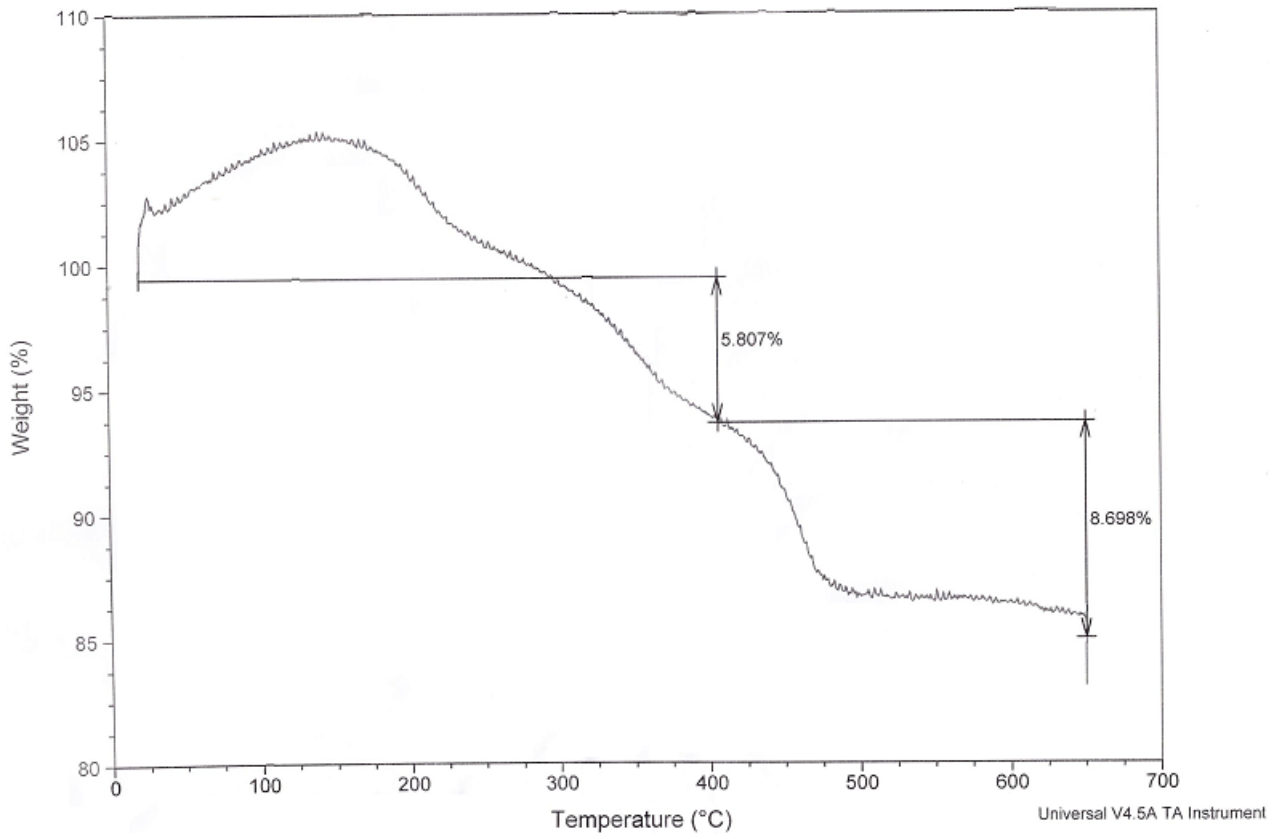

Figure 6. TGA analysis of fully reduced GO (~ 14% weight loss)

The TGA results show that GO flakes had the largest weight loss with 55% weight, followed by half reduced with 25% weight, and fully reduced with 14% weight. The percent weight loss depicts the loss of oxygen containing group on the surface of the GO. The TGA analysis of GO flakes and reduced GO shows a different weight percent loss due to different carbon to oxygen ratio of the nanoparticles.

2.4. Synthesis and Preparation of Epoxy nanocomposite films

Neat Film

The Seaguard HS 5000 amine Part A and epoxy hardener Part B were mixed in equivalent volume in a small vial and were mixed thoroughly. The mixture was then spread evenly onto a Teflon sheet and allowed to cure for two weeks (Neat film). The paint's wet weight and dry weight were measured and the dry weight was used for determining how much GO will be put into the film. Incorporating GO into the coating at 1 mg GO per 1 gram of butanol into the system made the mixture become too fluid and hard to spread onto the Teflon sheet, so the GO-butanol suspension was mixed with Part A of the paint and vacuumed through a hose at around 50 C to pull off excess butanol for around 2 hours. We then adopted a new method of incorporating GO-butanol of higher concentration of 5 mg/1g butanol, so that the excess butanol does not have to be evaporated off since the mixture was less fluid.

The most essential step in preparing the epoxy film was to not have any small bubbles form during the mixing, sonicating, or spreading onto the epoxy film as it results in uneven and porous film. The films were also peeled and turned over for faster curing and for easier handling when the film is flexible as it tends to get rigid and brittle after curing. The films were also given a mechanical pressure using weights on top to prevent any uneven surface or the bending of the film during curing. The films were given two weeks of time to cure before water vapor transmission testing.

2.5. Preparation for Water Vapor Transmission Test

The water vapor transmission rates were measured using ASTM E96-95: Methods for Water Vapor Transmission of Materials. The epoxy films were cut by razor blades into approximately 1.5 cm squares. About 3 to 5 samples were cut for each film made. The thicknesses of the samples were measured with a iGaging EZ-Cal digital micrometer with accuracy of 0.01 mm.

For each square sample, a 1.8 x 5.7 cm cylinder vial was filled up to 75 % with the desiccant Drierite with color indicator (Across Organics). The rim of the vial was coated with silicon vacuum grease and the films were placed firmly on top of the vial, creating a seal between the film and the vial to prevent the water vapor passage. Each vial was measured of their initial mass. The vials were then put into a humidity chamber with humidity of 75% in sealed environment at room temperature of 23^{o} C measured with Digital Temperature & Humidity Meter. A very convenient method to calibrate humidity sensors is the use of saturated salt solutions. At any temperature, the concentration of a saturated solution is fixed and does not have to be determined. By providing excess solute, the solution will remain saturated even in the presence of modest moisture sources and sinks. When the solute is a solid in the pure phase, it is easy to determine that there is saturation. Then the mass of each vials was measured over time up to 8~9 days. The rate of change of mass normalized by thickness versus time was used to calculate our relative water vapor transmission rate.

2.6. Water gain analysis

The procedure found in ASTM D750-98 standard test was used to determine the rate of water absorption. The epoxy film was cut into approximately 1 x 3 cm rectangular strips and their dimensions and thickness were recorded. The strip's initial mass was recorded and were submerged completely in deionized water and were kept at room temperature. Then measurements were made up to 3 days after submersion with 24-hour interval.

3. Results and Discussion

3.1. Permeability

A simple gas permeability model for a regular arrange of platelets was proposed by Nielsen [23] where the gas molecules pass through the film in the perpendicular direction to the evenly dispersed nanoplatelets, as shown in Figure 7.

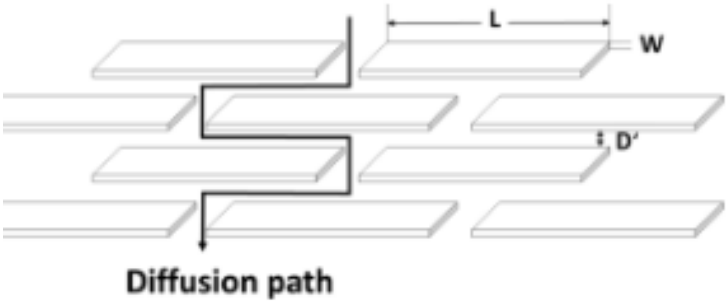

Figure 7.[24]

Choudalakis. G [24] have expanded the previous work done by Nielsen and have derived a simpler way to calculate the relative permeability of the nanocomposite. First, we can define <N> as the mean number of nanoplatelets a diffusing molecule encounters as it diffuses through the membrane and can be written as:

$$< \mathrm{N} > = l/W * \phi \quad (1)$$

where we define l as the thickness of the composite membrane, W as the thickness of the nanoplatelets, and ϕ as the volume fraction of the nanoplatelets that are dispersed in the polymer matrix. l/W can be viewed as the number of nanoplatelets it can be stacked in that membrane's thickness and ϕ accounts for the dispersion (or likelihood

of being in that stacked state) as a measure of volume fraction; the lower the volume fraction, the more dispersed the nanoplatelets are and the less nanoplatelets it will encounter during the diffusion.

The tortuous diffusion length (l') can be estimated as follows (labelled as diffusion path in Figure 7):[24]

$$l' = l + < N > * L/2 \quad (2)$$

Where L is the nanofiller's diameter or length. In this model, we assume the GO to be rectangular in shape and oriented perpendicular to the direction of gas diffusion; therefore, GO acts as a perfectly impermeable barrier against gas diffusion and that the nanoplatelets are arranged in a way that the edge of the above platelets is oriented to the middle of the bottom platelet as shown in Figure. 7.

We see that the diffusional path length in layered GO paper is significantly influenced by the GO platelet size: the impermeable nanoplatelet can create a tortuous, long pathway for the diffusing gas molecules. According to the solution–diffusion model, the gas permeability in polymer membranes can be expressed as a product of the diffusivity and solubility as follows:[25]

$$\mathrm{P} = \mathrm{D}\,\mathrm{S} \quad (3)$$

Where P is the gas permeability of the polymer, and D is the diffusivity of the gas molecule through the polymer membranes, and S is the solubility of the gas molecules in the membranes.

The solubility of the nanocomposites can be expressed as a function of the volume of the filler as follows:

$$S = S_o(1 - \phi) \quad (4)$$

Where S_o is the solubility of the pure polymer matrix and ϕ is the volume fraction of the nanoplatelets.

The diffusivity of nanocomposites, D, is influenced by the tortuosity τ:

$$D = \frac{D_o}{\tau} \quad (5)$$

Where D_o is the diffusivity of the polymer matrix itself and the τ is the tortuosity. The factor τ depends on the aspect ratio, the shape and the orientation of the nanoplatelets, and it is defined as:

$$\tau = l/l' \quad (6)$$

where l' is the tortuous pathways through the membrane and l is the membrane thickness, which is the shortest pathways for gas molecules, as shown in Figure 7.

Combining equation 3, 4, and 5, we get:

$$\frac{P}{P_o} = \frac{D\,S}{D_o S_o} = \frac{\frac{D_o}{\tau} * S_o(1-\phi)}{D_o S_o} = \left(\frac{1}{\tau}\right)(1 - \phi) = \frac{1-\phi}{\tau} \quad (7)$$

Where P_o is the permeability of the polymer matrix itself.

Substituting N into l' we have:

$$l' = l + \left(\frac{l}{W}\right)\phi * \frac{L}{2} = l\,(1 + \frac{\phi\, L}{2W}) \tag{8}$$

Then substituting l' into the tortuosity (equation 8 into 6), τ can be rewritten as:

$$\tau = 1 + \frac{\phi\, L}{2W} \tag{9}$$

Combining equation 7 and 9, we can express the relative permeability as:

$$\frac{\mathrm{P}}{\mathrm{P_o}} = \frac{1-\phi}{1+(\frac{\alpha}{2}*\phi)} \tag{10}$$

Where we now define $\alpha = \frac{L}{W}$ or as an aspect ratio of the nanoplatelets. This equation shows that the permeability of the nanocomposite decreases with the increase of ϕ and α.

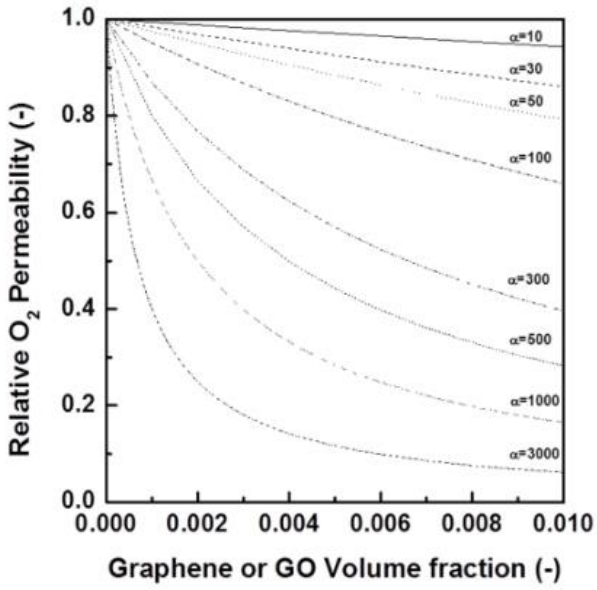

Figure 8. Predictions of Nielsen's model for the relative permeability as a function of different aspect ratio [24]

From the work by Choudalakis, G[24], we can see the predicted the O_2 gas permeability reduction with varying aspect ratio using the Nielsen model as shown in Figure 8. The graph clearly shows that the aspect ratio plays a crucial role in the reducing the permeability with an increasing tortuosity effect. If we assume that the GO Volume fraction to be equal to percent weight, at a 0.5 % weight loading, with an aspect ratio of 1000, we would see 0.3 relative permeability or 70 % reduction in permeability. However, this model is an approximation and it assumes that nanofillers are perfectly oriented perpendicular to the diffusion path.

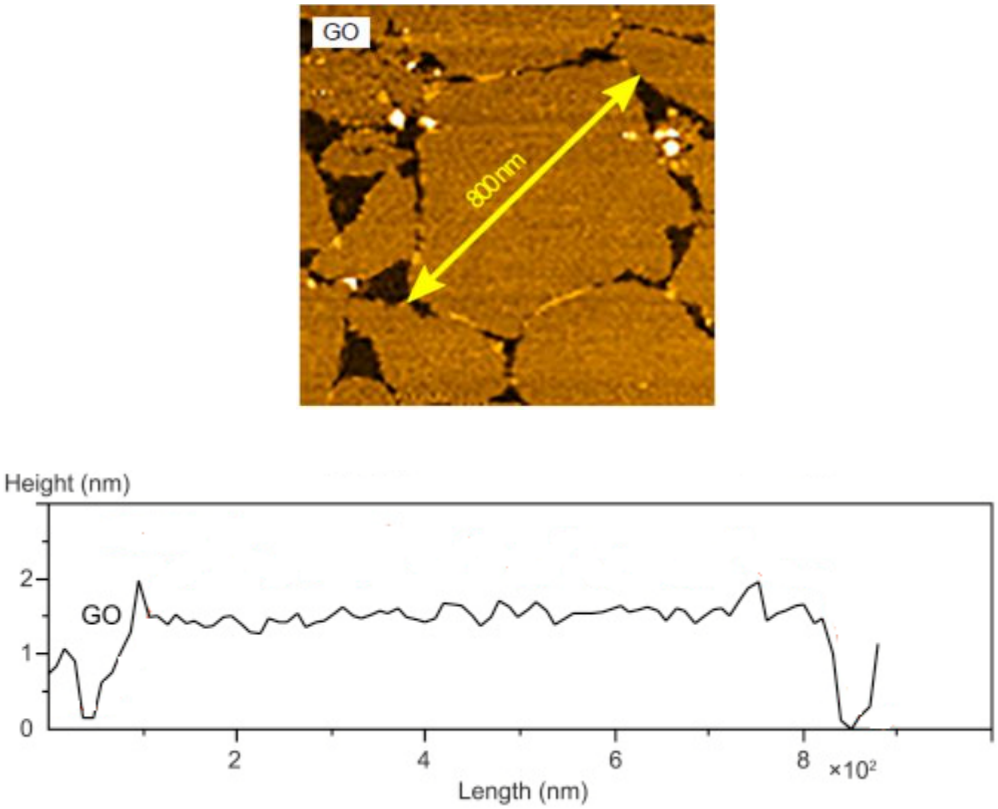

Figure 9. Atomic force microscope image of graphene oxide (GO)

Previous work done by Hocker, S in our lab have confirmed the size of the GO using the atomic force microscope. From the image, we determined the aspect ratio to be around 500 to 1000 assuming that the GO nanoparticle's length to be around 500 to 1000 nm and the thickness to be from 1 to 2 nm. [25]

3.2 Water Vapor Transmission Results

The water vapor transmission was calculated as follows. Three to five samples were cut out of the one film and their weight change over days were recorded. The measurement time was kept consistent as well as the balance. The weight gained was multiplied by the thickness of the sample for normalization. Then it was divided by the number of days it was in the humidity chamber. Approximately four to five measurements were made during the course of 8~10 days. The four to five measurements' value now will have the unit of : weight gained * thickness per day. Then I averaged the weight gain per sample and the standard deviation was calculated. Then I averaged the samples that were cut from the same film.

Note: Any samples that had weight change more than 5 mg between the measurements were discarded in calculating the average, because this indicates a bad seal.

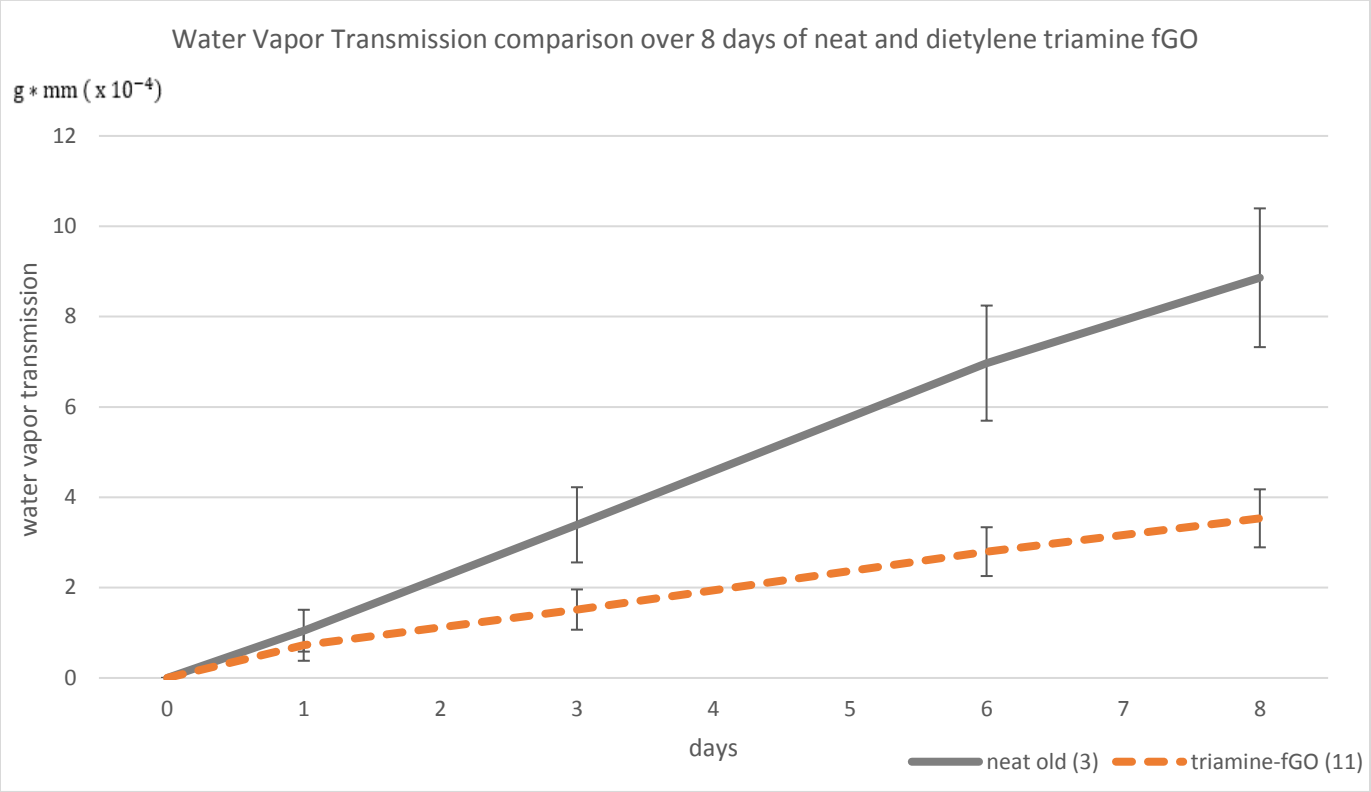

Fig. 10 Example of Water Vapor Transmission of Neat film and diethylene-triamine fGO over 8 days

The number in parenthesis represents number of samples used in calculating the average. In the Figure 10, we can confirm the linear mass gain for the different films during the measurements over 8 days and calculate mass gain per day per sample by calculating the slope.

*The tabulated data that were used to make the graph can be found in the Appendix.

Table1. Sonicated	Average permeability (g*mm)/days (x10^-4)
neat average (20)	1.035
0.01 HrGO (1)	0.566
0.05 HrGO (1)	0.654
0.1 HrGO (5)	0.864
0.01 FrGO (2)	0.750
0.05 FrGO (0)	
0.1 FrGO (5)	0.450

Table 2. Stirred	Average permeability (g*mm)/days (x10^-4)
neat average (20)	1.035
0.01 HrGO (1)	0.911
0.05 HrGO (2)	1.404
0.1 HrGO (5)	0.467
0.01 FrGO (1)	0.389
0.05 FrGO (2)	0.458
0.1 FrGO (5)	0.598

Table 3. Stirred (reduced Butanol)	Average permeability (g*mm)/days (x10^-4)
neat average (20)	1.035
HrGO 0.01 (3)	0.781
HrGO 0.05 (3)	3.133
HrGO 0.1 (2)	0.483
FrGO 0.01 (2)	1.638
FrGO 0.05 (3)	1.127
FrGO 0.1 (3)	1.061

As seen in Tables 1,2 and 3, we saw no detectable effect of nanoparticle's concentration in reducing the water vapor transmission. Increasing the concentration by factor of 10 had no significant effect. For different methods of dispersion and different functionalization, we did not see 0.1 weight % loading producing consistently better results than the lower loadings of 0.05 weight % and 0.01 weight %. We propose that this might be due uneven dispersion, particle agglomeration/poor exfoliation of particles, or that the nanoparticles were incorporated at such low weight percent to not be able to detect measurable effects between the different loadings.

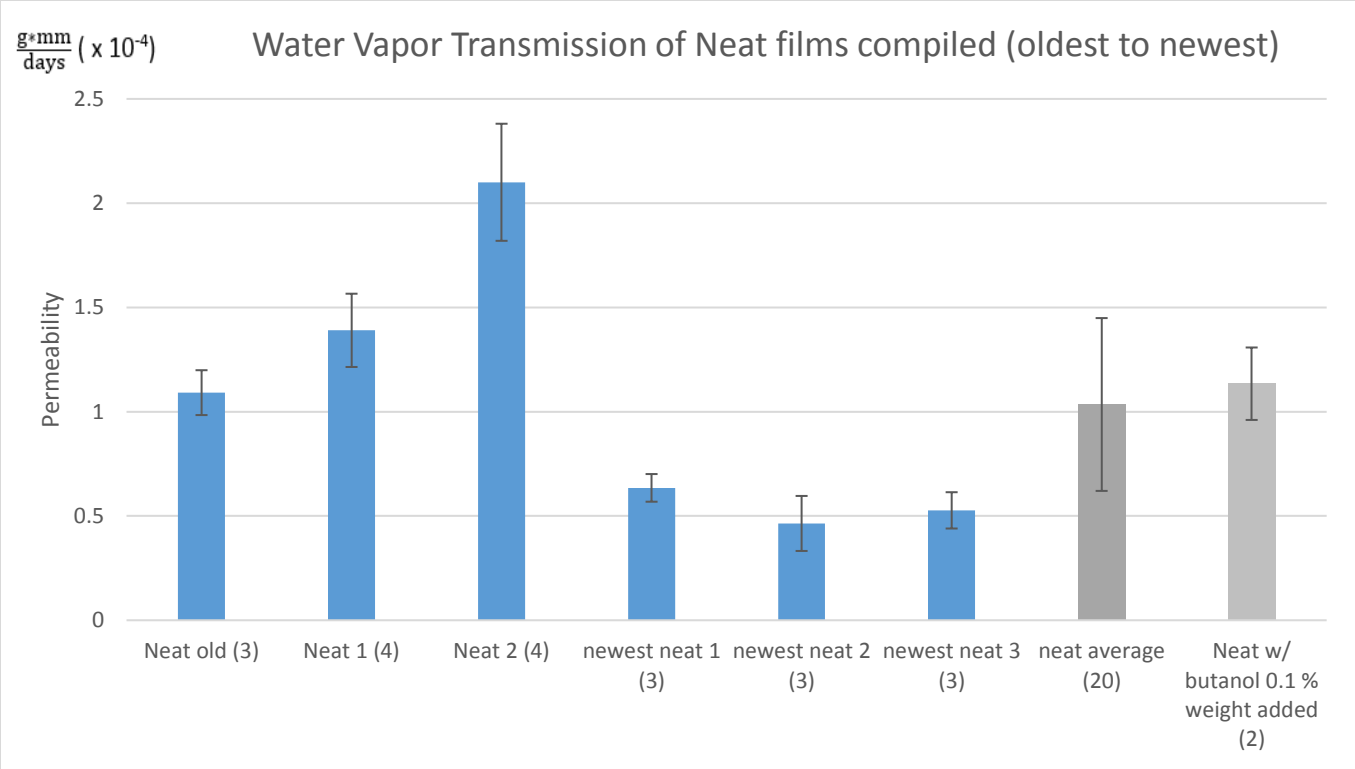

Figure 11. Water Vapor Transmission comparison for the neat films

To minimize the variability within the same type of film and to set a baseline for comparison, the neat films were synthesized 6 times in total. However, we still saw variability among the 6 films even after discarding the leaked or bad samples. In Figure 11, the films are listed from oldest to newest left to right. Out of 6 different neat films, 20 samples were ended up being used to calculate the average of the neat.

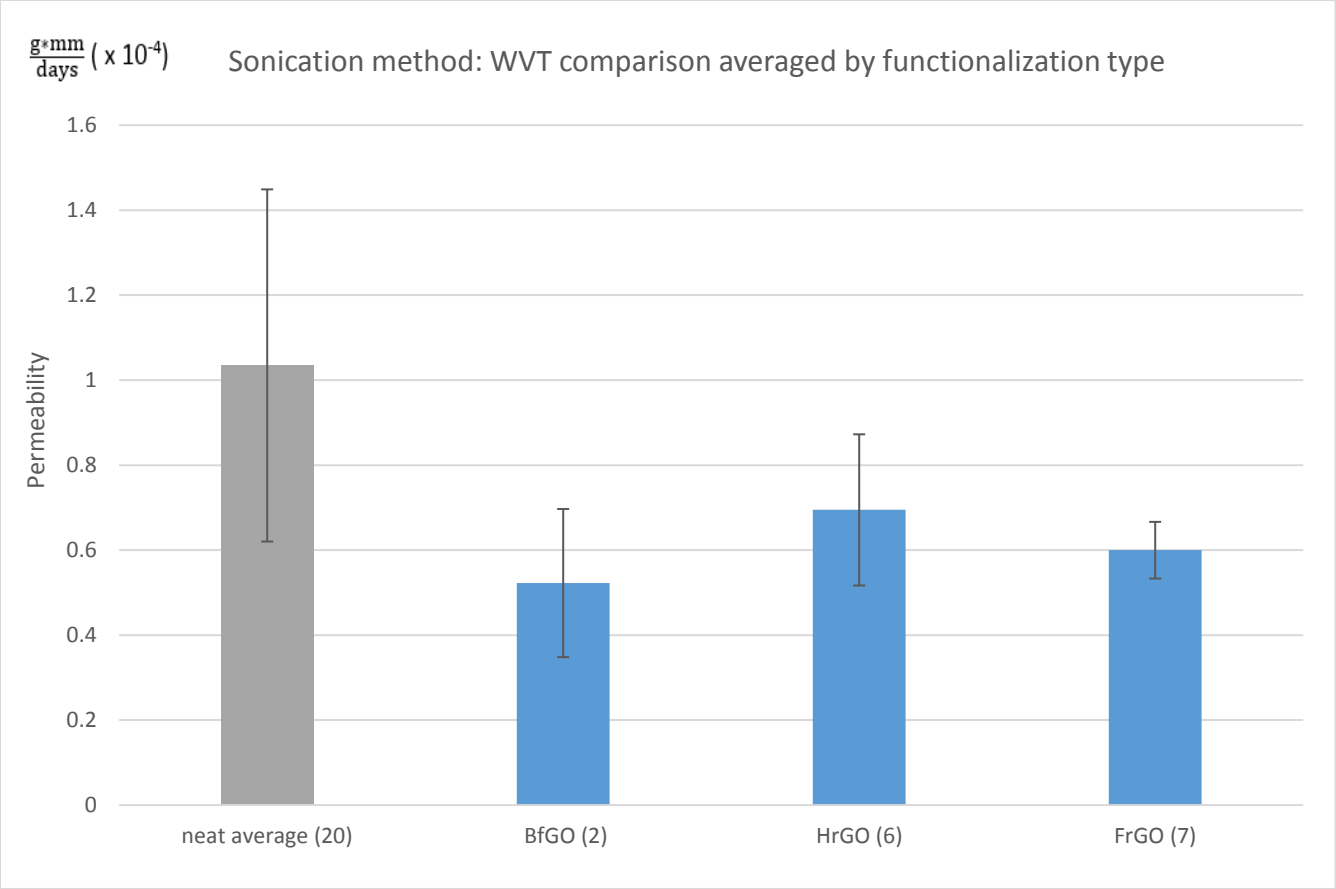

Figure 12. Water Vapor Transmission comparison between the Sonicated.

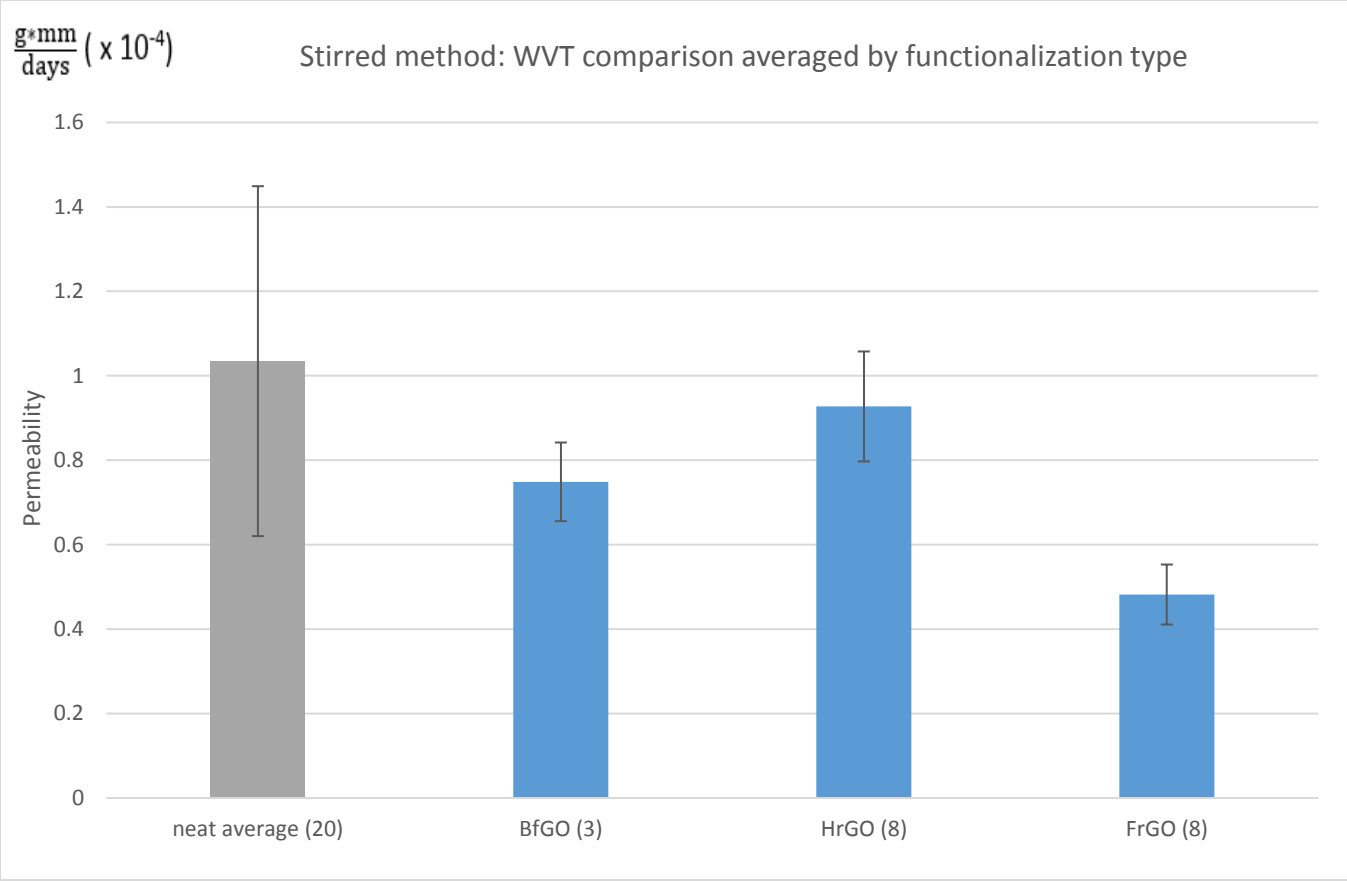

Figure 13. Water Vapor Transmission comparison between the Stirred samples.

For the sonication method, we were able to achieve about a 50% reduction in water vapor permeability for the butyl-amine functionalized GO compared to the neat and around 30 to 40% decrease for the Half and Fully reduced GO. However, we do not have the statistical evidence to support that butyl-functionalized GO had the best improvement.

For the stirring method on the other hand, we were able to achieve 50% decrease for the Fully reduced GO and around 15 to 25 % decrease for half reduced and butyl amine functionalized GO.

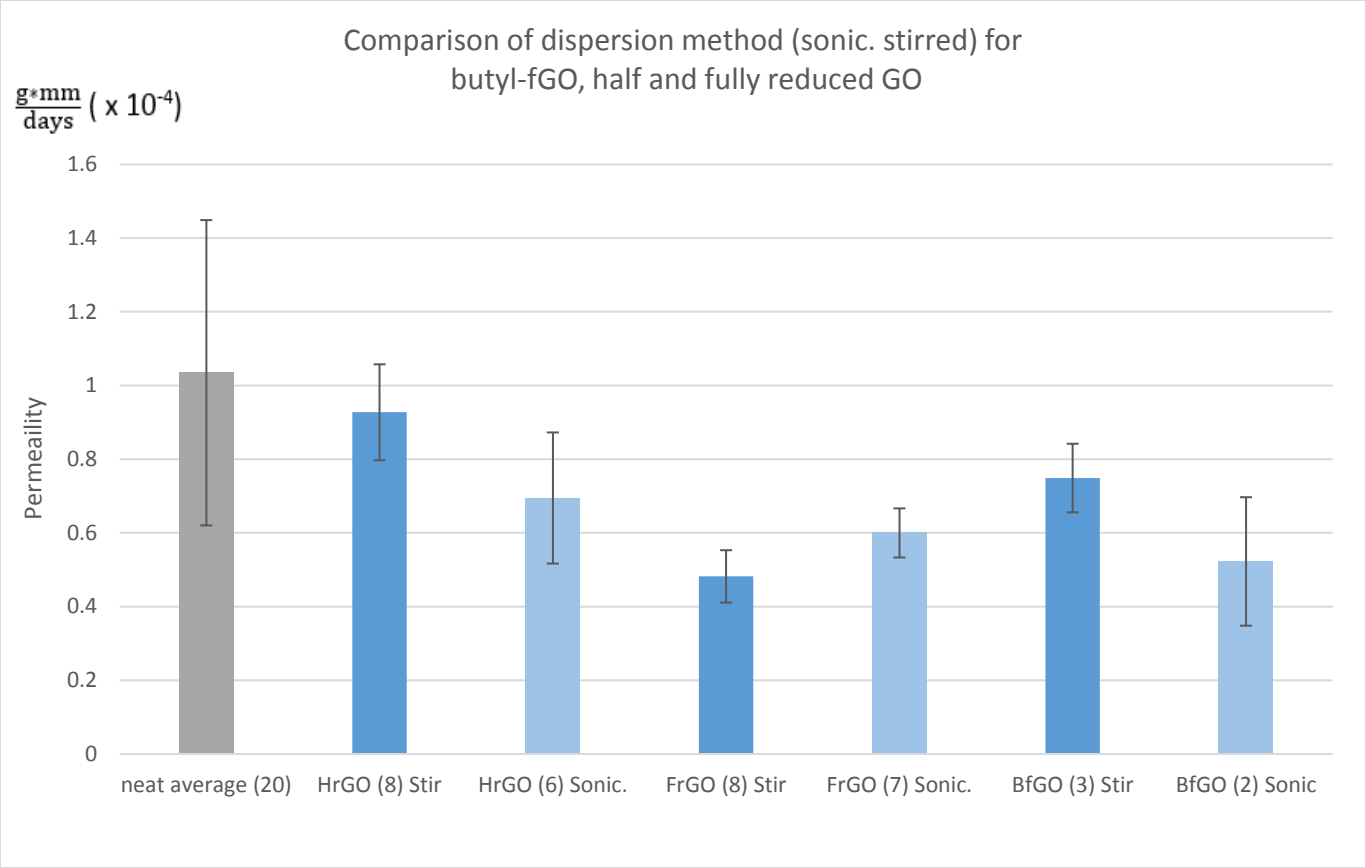

Figure 14. Comparison between the two different dispersion method.

Based on the results, fully reduced shows better results when stirred whereas half reduced and butyl-amine fGO was better when sonicated. This is the opposite of my initial hypothesis that fully reduced GO might be better if sonicated being more susceptible to agglomeration therefore requiring higher power of mixing to evenly disperse. However, we still should consider if the result is due to the effect of different mixing or the different modification of the GO.

However, when averaged, the stirred method of both half and fully reduced GO gives a value of 0.0000764 whereas average of the sonicated for both half and fully reduced GO had value of 0.0000811. The butyl-amine fGO shows a better result with the

sonication method. Here we can conclude that the sonication method has greater effect in reducing the permeability overall. We can further conclude that the state of dispersion might have bigger effect than the nanoparticle sizes in reducing the permeability.

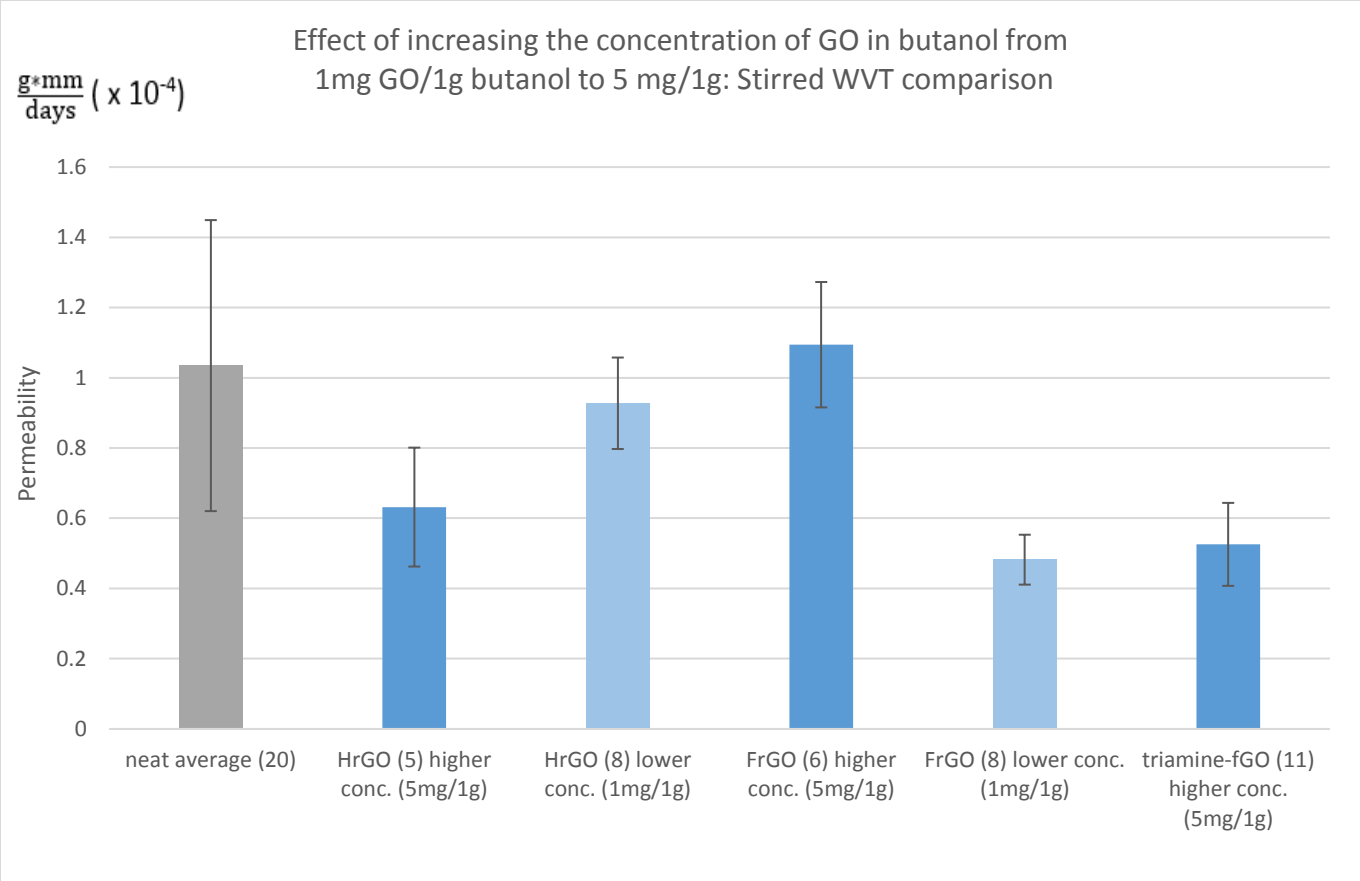

Figure 15. Effect of increasing the GO concentration in butanol by 5 times.

For the films in the previous two graph, the GO were suspended in butanol at a concentration of 1 mg GO per 1 g of butanol. As stated in the experimental section, when lower concentration of GO / butanol suspension was added to the Part A paint, the mixture became too fluid. To ease the processing and curing of the films, the concentration of GO in the butanol was increased to 5 mg per 1 g of butanol and we wanted to study the if incorporating at a higher concentration had any effect on the water permeability. Here, the new functionalization was tried with the diethylene-triamine and showed the best result with about 50% reduction and Half reduced showed about 40%.

As for the effect of changing the concentration, Fully reduced seemed to work better at the lower concentration in butanol and for half reduced concentration, the higher concentration seemed to work better. This may be due to the nanosheets being agglomerated when the graphene oxide is fully reduced as the removal of oxygen containing group made the sheets hydrophobic. This causes them to agglomerate and not be well dispersed. Whereas half reduced still retained the oxygen functional group to be able to be dispersed well at a higher concentration.

3.3. Water Gain Analysis

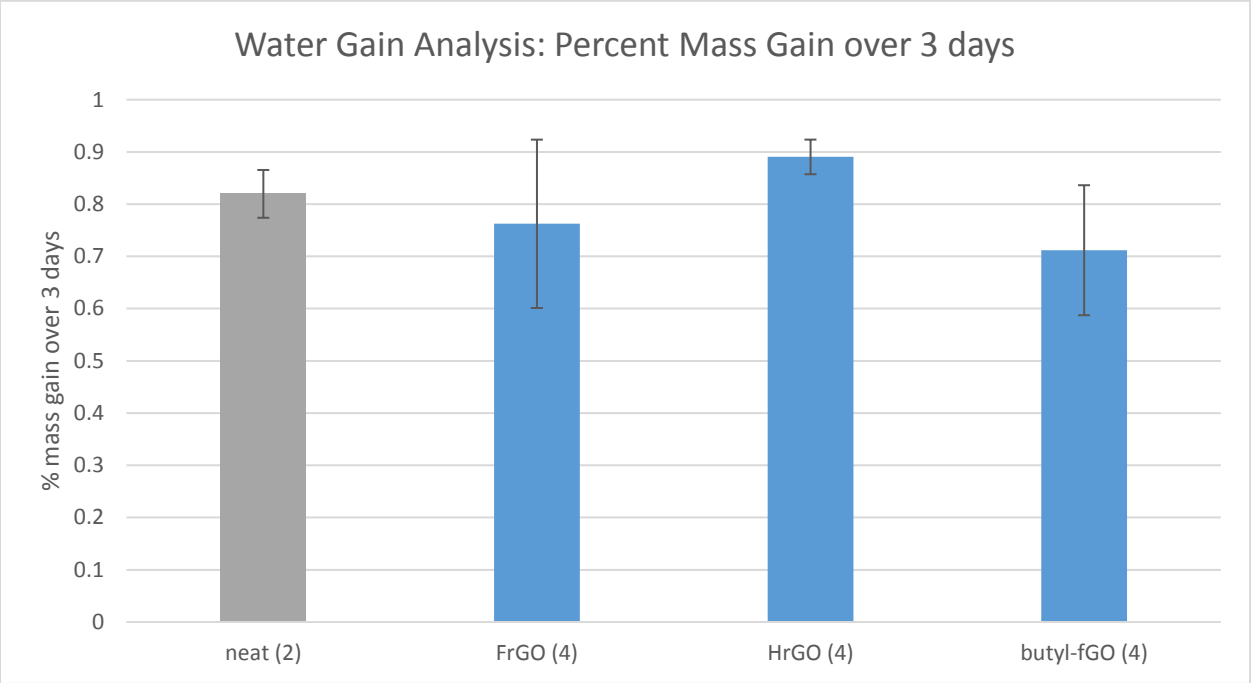

Figure 16. Water Gain Analysis comparison

As seen in Fig. 9, only the fully reduced and the butyl-amine functionalized showed slightly less water absorption compared to the neat sample of around 12 % less for the butyl-amine fGO. The water absorbed for the strips were less than 2 mg over 24 hours and remained the same weight after the first measurement at 24 hours.

4. Conclusion

Improvement in reduction of water vapor transmission is possible even at a very low GO weight loadings of 0.01 to 0.1 weight percent, with a reduction of about 50 percent compared to the neat film. At such low concentration, we saw no measurable effect between the different weight loadings of GO in the epoxy film.

Different functionalization or surface effect of the GO had a significant effect. The diethylene-triamine showed the best and most consistent result with approximately 50% water vapor permeability reduction, followed by butyl-amine functionalized with 35% reduction, fully-reduced with 33 % reduction to half reduced GO with 25 % reduction. The important step is selecting a functionalizing molecule that readily reacts with the epoxy groups or carboxyl group of the surface of the GO and that could also react or form a strong intermolecular force between the GO nanosheets and the polymer. The resulting increase in nanoparticle-polymer interaction has the potential to stiffen and restrict the mobility of the polymer chain, further enhancing the tortuosity effect. This latter point will be explored by dynamic modulus torsion experiment.

In comparing the different methods of dispersing the GO, even though the stirring method allowed to retain a bigger particle size and aspect ratio, the sonication method had better overall effect in reducing the water vapor permeability. We speculate that the exfoliation and dispersion state for the graphene nanosheet in the polymer matrix is a more significant than the structure of the graphene itself such as particle sizes or high aspect ratio.

The water gain analysis showed the biggest decrease in water absorption for the butyl-amine fGO of approximately 13% and fully reduced GO of approximately 10% compared to the neat. For water absorption as well as water vapor transmission, these results show that by functionalizing the surface of the GO, we can enhance the interaction between the polymer and the nanoparticle. This reduces and restricts the mobility of the polymer chains and its ability to absorb water and transmit water vapor even at a very low loading of 0.10 weight% or less.

Our future work includes finding the optimal concentration the GO that can be suspended in the solvent and put into the epoxy paint without excess butanol, further confirming the better effect of well-dispersed GO nanoparticles over the particle size by making films with sonicated GO, and performing mechanical tests on the previous and newly made samples to verify the nanoparticle's effect on polymer chain mobility.

References

1. Nurxat Nuraje, Shifath I. Khan, Heath Misak, and Ramazan Asmatulu, “The Addition of Graphene to Polymer Coatings for Improved Weathering,” ISRN *Polymer Science*, vol. 2013, Article ID 514617, 8 pages, 2013. doi:10.1155/2013/514617

2. B.M. Yoo, H.J. Shin, H.W. Yoon, H.B. Park “Graphene and graphene oxide and their uses in barrier polymers” J. *Appl. Polym. Sci.*, 131 (1) (2014), p. 39628

3. Yanbin Cuia, S.I. Kundalwalb, 1, S. Kumar. “Gas barrier performance of graphene/polymer nanocomposites.,” *Carbon*, Volume 98, March 2016, Pages 313–333

4. Caterina Soldano, Ather Mahmood1, Erik Dujardin. “Production, properties and potential of graphene,” *Carbon,* Volume 48, Issue 8, July 2010, Pages 2127–2150

5. Md J. Nine, Martin A. Cole, Lucas Johnson, Diana N. H. Tran, and Dusan Losic. “Superhydrophobic Graphene-Based Composite Coatings with Self-Cleaning and Corrosion Barrier Properties,” *Applied Materials and Interfaces* p. 28482-28491

6. Y. Su, V. G. Kravets, S. L. Wong, J. Waters, A. K. Geim, R.R. Nair. “Impermeable Barrier Films and Protective Coatings Based on Reduced Graphene Oxide,”*Nature*. Sept 2014, p. 1-10

7. B. Ahmadi-Moghadam, M. Sharafimasooleh, S. Shadlou, F. Taheri. “Effect of functionalization of graphene nanoplatelets on the mechanical response of graphene/epoxy composites” *Materials and Design*. Volume 66, Part A, 5 February 2015, Pages 142–149

8. Tapas Kuilaa, Saswata Bosea, Ananta Kumar Mishrab, Partha Khanraa, Nam Hoon Kimc, Joong Hee Leea, “Effect of functionalized graphene on the physical properties of linear low density polyethylene nanocomposites” *Polymer Testing,* Volume 31, Issue 1, February 2012, Pages 31–38

9. Tapas Kuilaa, Saswata Bosea, Ananta Kumar Mishrab, Partha Khanraa. “Chemical functionalization of graphene and its applications,” *Progress in Materials Science,* Volume 57, Issue 7, September 2012, Pages 1061–1105

10. Kim, Seong Woo; Choi, Hyun Muk. “Morphology, thermal, mechanical, and barrier properties of graphene oxide/poly(lactic acid) nanocomposite films,” *Korean Journal Of Chemical Engineering,* Vol 33 Issue 1, 2016. p.330-336.

11. Morimune, S.; Nishino, T.; Goto, T., Ecological Approach to Graphene Oxide Reinforced Poly(methyl methacrylate) Nanocomposites. *ACS Aplied Materials & Interface* 2012, 4 (7), 3596-3601

12. Zhu, J.; Lim, J.; Lee, C. H.; Joh, H. I.; Kim, H. C.; Park, B.; You, N. H.; Lee, S., Multifunctional polyimide/graphene oxide composites via in situ polymerization. *Journal of Applied Polymer Science* 2014, 131 (9).

13. Jin, J.; Rafiq, R.; Gill, Y. Q.; Song, M., Preparation and characterization of high performance of graphene/nylon nanocomposites. European Polymer Journal 2013, 49 (9), 2617-2626.

14. Yang, J.; Bai, L.; Feng, G.; Yang, X.; Lv, M.; Zhang, C. a.; Hu, H.; Wang, X., Thermal Reduced Graphene Based Poly(ethylene vinyl alcohol) Nanocomposites: Enhanced Mechanical Properties, Gas Barrier, Water Resistance, and Thermal Stability. *Industrial & Engineering Chemistry Research* 2013, 52 (47), 16745-16754

15. Priolo, M. A.; Gamboa, D.; Holder, K. M.; Grunlan, J. C. Super Gas Barrier of Transparent Polymer-Clay Multilayer Ultrathin Films. *Nano* Lett. 2010, 10, 4970.

16. Jacquelot, E.; Espuche, E.; Gérard, J. F.; Duchet, J.; Mazabraud, P. J. Polym. Sci. Part B: *Polym*. Phys. 2005, 44, 431.

17. Azeredo, H. M. C. D. *Food Res*. Int. 2009, 42, 1240.

18. Arora, A.; Padua, G. W. J. *Food Sci.* 2010, 75, R43.

19. Park, J. S.; Chae, H.; Chung, H. K.; Lee, S. I. Semicond. Sci. *Techno*l. 2011, 26, 034001

20. Hu, A.; Guo, J.; Alarifi, H.; Patane, G.; Zhou, Y.; Compagnini, G.; Xu, C. *Appl. Phys*. Lett. 2010, 97, 153113.

21. Lange, J.; Wyser, Y. *Packaging Technol*. Sci. 2003, 16, 149

22. Hummers, W. S.; Offeman, R. E. J. *Am. Chem. Soc*. 1958, 80, 1339.

23. Nielsen, L. E. J. Macromol. *Sci*. Chem. 1967, 1, 929.

24. Choudalakis, G.; Gotsis, A. Eur. *Polym*. J. 2009, 45, 967.

25. Gorrasi, G.; Tammaro, L.; Tortora, M.; Vittoria, V.; Kaempfer, D.; Reichert, P.; Mülhaupt, R. J. Polym. Sci. Part B: Polym. Phys. 2003, 41, 1798.

26. Samuel Hocker, Natalie Hudson-Smith, Hannes C. Schniepp, David E. Kranbuehl *Polymer* 2016 93, 23-29

27. Gotro Jeffrey. Epoxy Cure Chemistry Part 4. March, 2014